



PAPER • OPEN ACCESS

Comments on the fractal energy spectrum of honeycomb lattice with defects

To cite this article: Yoshiyuki Matsuki and Kazuki Ikeda 2019 *J. Phys. Commun.* **3** 055003

View the [article online](#) for updates and enhancements.

You may also like

- [Fractal Dimension of Electrochemical Reactions](#)
Ali Eftekhari
- [Synchrosqueezed wavelet transform-fractality model for locating, detecting, and quantifying damage in smart highrise building structures](#)
Juan P Amezcuita-Sanchez and Hojjat Adeli
- [Emergence of fractal geometry on the surface of human cervical epithelial cells during progression towards cancer](#)
M E Dokukin, N V Guz, C D Woodworth et al.



PAPER

OPEN ACCESS

RECEIVED
26 March 2019

REVISED
31 March 2019

ACCEPTED FOR PUBLICATION
12 April 2019

PUBLISHED
8 May 2019

Original content from this work may be used under the terms of the [Creative Commons Attribution 3.0 licence](#).

Any further distribution of this work must maintain attribution to the author(s) and the title of the work, journal citation and DOI.



Comments on the fractal energy spectrum of honeycomb lattice with defects

Yoshiyuki Matsuki and Kazuki Ikeda

Department of Physics, Osaka University, Toyonaka, Osaka 560-0043, Japan

E-mail: kikeda@het.phys.sci.osaka-u.ac.jp

Keywords: Hofstadter butterfly, defect, energy spectra

Abstract

We study the fractality of the energy spectrum of honeycomb lattice with various defects or impurities under a perpendicular magnetic field. Using a tight-binding Hamiltonian including interactions with the nearest neighbors, we investigate its energy spectrum for different choices of point defects or impurities. First, we fix a unit cell consisting of 8 lattice points and survey the energy eigenvalues in the presence of up to 2 point defects. Then it turns out that the existence of the fractal energy structure, called Hofstadter's butterfly, highly depends on the choice of defect pairs. Next, we extend the size of a unit cell which contains a single point defect in the unit cell consisting of 18 and 32 lattice points to lower the density of the defects. In this case, the robust gapless point exists on the $E = 0$ eV line without depending on the size of unit cells. And we find this gapless point always exists at the center of the butterfly shape. This butterfly shape also exists for the case of no defect lattice which has the fractality.

1. Introduction

It has been widely known that the graph of the spectrum over a wide range of rational magnetic fields passing through a two-dimensional lattice shows fractal, called the Hofstadter butterfly [1], which is confirmed by various experimental studies [2–4]. This intriguing behavior of Bloch electrons has long attracted the major interest of researchers from various perspectives. In a two-dimensional system, the Hofstadter problem is addressed for various choice of lattices: general Bravais lattice [5], buckled graphene like materials [6] and square lattice with next-nearest-neighbor hopping [7]. More recently Hofstadter's butterfly appears in relation to the quantum geometry [8, 9] and it is also surveyed from a perspective of mathematical physics [10–12]. This problem is extended to higher dimensional cases [13–15] and it is known that analog of Hofstadter's butterfly exists in more general systems. Yet, the underlying theoretical reasons of such fractality has not been clear.

All of the above theoretical studies are based on the perfect lattice structures, therefore it would be natural to consider the problem: does the fractal structure appear on various lattice systems with defects? Indeed, there are some authors worked on this issue. For example, a square lattice with an array of point defects was studied in [16], and Hall conductance in graphene with point defects was studied in [17]. As well as investigating the origin of the fractal nature, we aim at giving a positive answers for this question. Apparently it is a formidable task to find such a fractal energy spectrum in a system with defects or impurities since they usually make energy bands gapped. Indeed, as we report in this article the energy spectrum highly depends on a choice of defect pairs and analog of the Hofstadter butterfly exists only under appropriate conditions. It is briefly reported that the honeycomb lattice with a single point defect in a unit cell accommodates the fractal spectrum with large band gaps nearby the $E = 0$ eV line (figure 3) and point defects are responsible for modifying the Hofstadter butterfly structure [18]. As a succeeding study, we investigate more on influence of defects or impurities on the energy spectrum in order to enhance our knowledge on its fractal nature. Though it is obvious that the fractal structure cannot be obtained if too many defects are introduced into a unit cell, as a

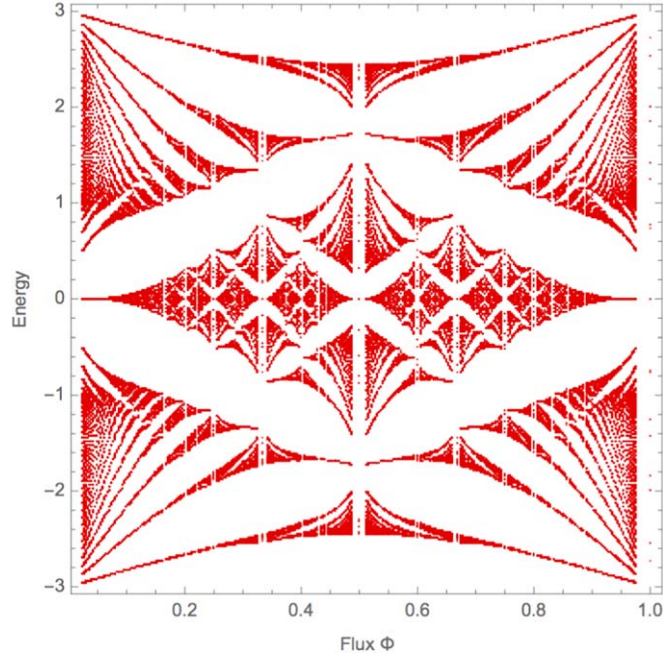


Figure 1. Energy spectrum plotted over a wide range of ϕ on a pure honeycomb lattice.

non-trivial result, we find that the large band gaps reported in the previous paper [18] are closed and the graph of the energy spectrum looks like symmetric rather than fractal when another atom is vacant so that the honeycomb lattice accommodates line defects (figure 4). In addition, even for several enlarged unit cells, we observe a robust gapless point on the $E = 0$ eV line that exists without depending on the size of a unit cell. It can be found at the center of the butterfly shape ($\phi = 0.5$ in figure 1) and it is crucial to the fractal nature of the graph.

This article is orchestrated as follows. In section 2 we explain our problem setting. We use the tight-binding Hamiltonian including the nearest neighbor interactions of electrons in enlarged unit cells with point defects or impurities. In section 3, we present a number of graphs obtained by numerical calculation for various choices of defects and for several enlarged unit cells. We also give several theoretical reasons for the obtained family of energy structures and consider the origin of the fractal nature in various setups. This article is concluded in section 4 with some proposed future works.

2. Model and formulation

Here we explain our model used for this article. We introduce the effect of the magnetic field into the 2 dimensional honeycomb lattice system by the Peierls substitution [19]

$$|\mathbf{R}_i\rangle\langle\mathbf{R}_j| \rightarrow e^{i\Theta_{ji}^{mag}} |\mathbf{R}_i\rangle\langle\mathbf{R}_j|, \quad (1)$$

where $\Theta_{ji}^{mag} = -\frac{e}{\hbar} \int_{\mathbf{R}_j}^{\mathbf{R}_i} \mathbf{A} \cdot d\mathbf{l}$. In the Landau gauge $(0, Bx, 0)$, it corresponds to

$$\Theta_{ji}^{mag} = -\pi \frac{\phi}{S} ((\mathbf{R}_j + \mathbf{R}_i) \cdot \hat{x}) ((\mathbf{R}_i - \mathbf{R}_j) \cdot \hat{y}), \quad (2)$$

where \mathbf{R}_i is a position vector specifying the atom, $\mathbf{R}_i = m_\alpha^i \mathbf{a}_1 + n_\alpha^i \mathbf{a}_2$ with labels α of the atoms in the enlarged unit cell i , $\phi = BS/\phi_0$, $\phi_0 = h/e$ and S is the area of the enlarged unit cell.

Under this setup, our system can be written by means of a new matrix equation which can be called the generalized Harper equation [20]

$$E\Psi_m = U_m\Psi_m + V_m\Psi_{m+1} + W_m\Psi_{m-1}. \quad (3)$$

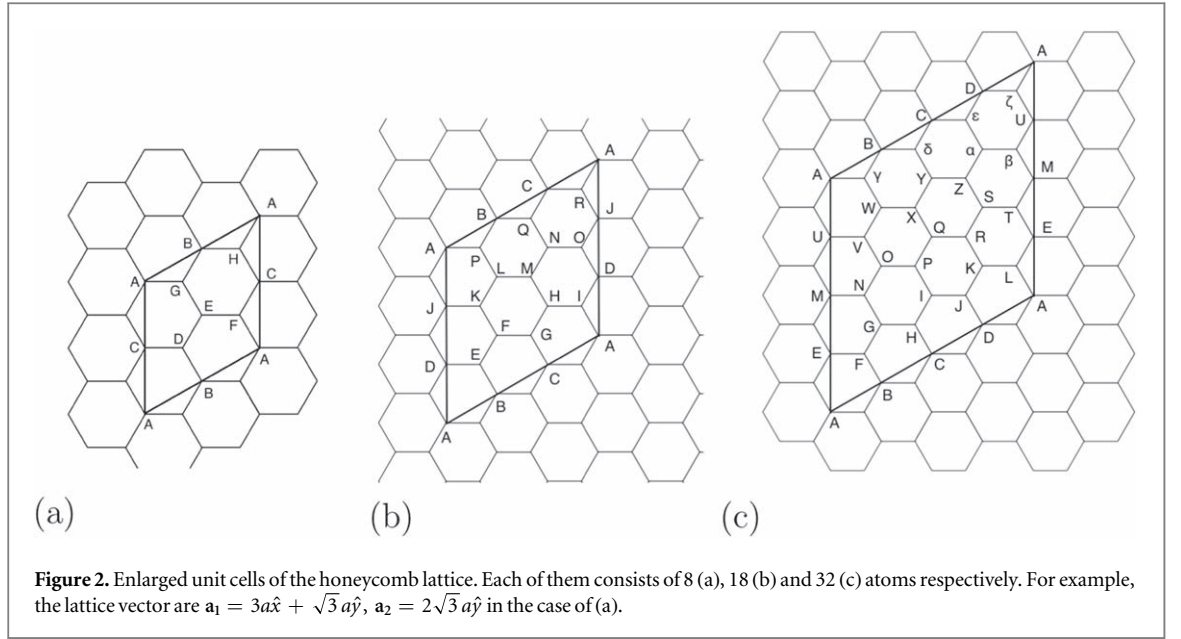


Figure 2. Enlarged unit cells of the honeycomb lattice. Each of them consists of 8 (a), 18 (b) and 32 (c) atoms respectively. For example, the lattice vector are $\mathbf{a}_1 = 3a\hat{x} + \sqrt{3}a\hat{y}$, $\mathbf{a}_2 = 2\sqrt{3}a\hat{y}$ in the case of (a).

Using matrix representation, we rewrite it as

$$E \begin{bmatrix} \Psi_1 \\ \Psi_2 \\ \vdots \\ \Psi_{q-1} \\ \Psi_q \end{bmatrix} = \begin{pmatrix} U_1 & V_1 & 0 & 0 & \dots & 0 & W_1^* \\ W_2 & U_2 & V_2 & 0 & 0 & \dots & 0 \\ 0 & W_3 & U_3 & V_3 & 0 & \dots & 0 \\ \vdots & \vdots & \ddots & \ddots & \ddots & \dots & \vdots \\ V_q^* & 0 & 0 & \dots & 0 & W_q & U_q \end{pmatrix} \begin{bmatrix} \Psi_1 \\ \Psi_2 \\ \vdots \\ \Psi_{q-1} \\ \Psi_q \end{bmatrix}, \quad (4)$$

where U_m, V_m, W_m are certain matrixes and $W_1^* = W_1 e^{-ik_x a_{1x} q}$, $V_q^* = V_q e^{-ik_x a_{1x} q}$ ($-\frac{\pi}{q} \leq k_x \leq \frac{\pi}{q}$, $-\pi \leq k_y \leq \pi$). Note that the index m is periodic in q with a period q therefore wave functions are written

$$\psi_{m+q} = e^{ik_x a_{1x} q} \psi_m \quad (5)$$

by Bloch's theorem. For example, if the unit cell (a) in figure 2 is preferred, then Ψ_m has the form

$$\Psi_m = \begin{bmatrix} \psi_m^A \\ \psi_m^B \\ \psi_m^C \\ \psi_m^D \\ \psi_m^E \\ \psi_m^F \\ \psi_m^G \\ \psi_m^H \end{bmatrix} \quad (6)$$

and U_m, V_m, W_m are 8×8 matrixes. Then solving the characteristic equation $\det(E - H) = 0$ with respect to each ϕ , where H is defined by the right hand side of the equation (4), we obtain the butterfly shape (figure 1).

We investigate that the energy spectra dependence on position of impurities or defects in the honeycomb lattice whose unit cell is displayed figure 2(a), and dependence on the density of defects by changing the size of a unit cell (figure 2). In the first study, we treat the atom at E as a defect and introduce additional impurities at C, F and H , respectively. (Those three pairs are enough for our purpose since the honeycomb lattice has the $\pi/6$ rotation symmetry as well as the transition symmetry.) (E, F) is a nearest neighbor pair of defects, (E, C) is a next-nearest neighbor pair of defects, and (E, H) is a third nearest neighbor pair of defects. In the second study, each unit cell (from (a) to (c) in figure 2) contains a single defect (E in (a), L in (b) and Q in (c)), and the purity of the honeycomb lattice would get close to a realistic situation (the density of defect 0.125 (a), 0.056 (b), 0.031 (c)). Throughout this article, all interactions among Bloch electrons are treated as the nearest neighbor interactions.

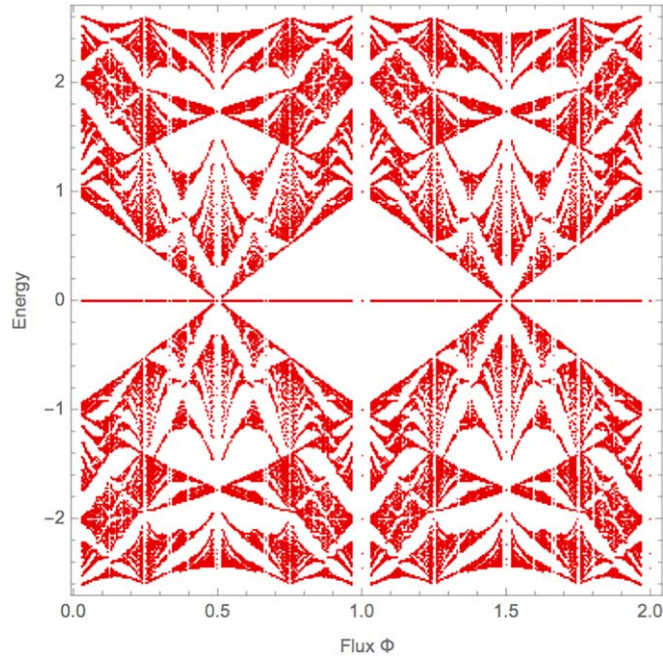


Figure 3. Spectrum for a honeycomb lattice whose unit cell has a single defect.

3. Results and discussion

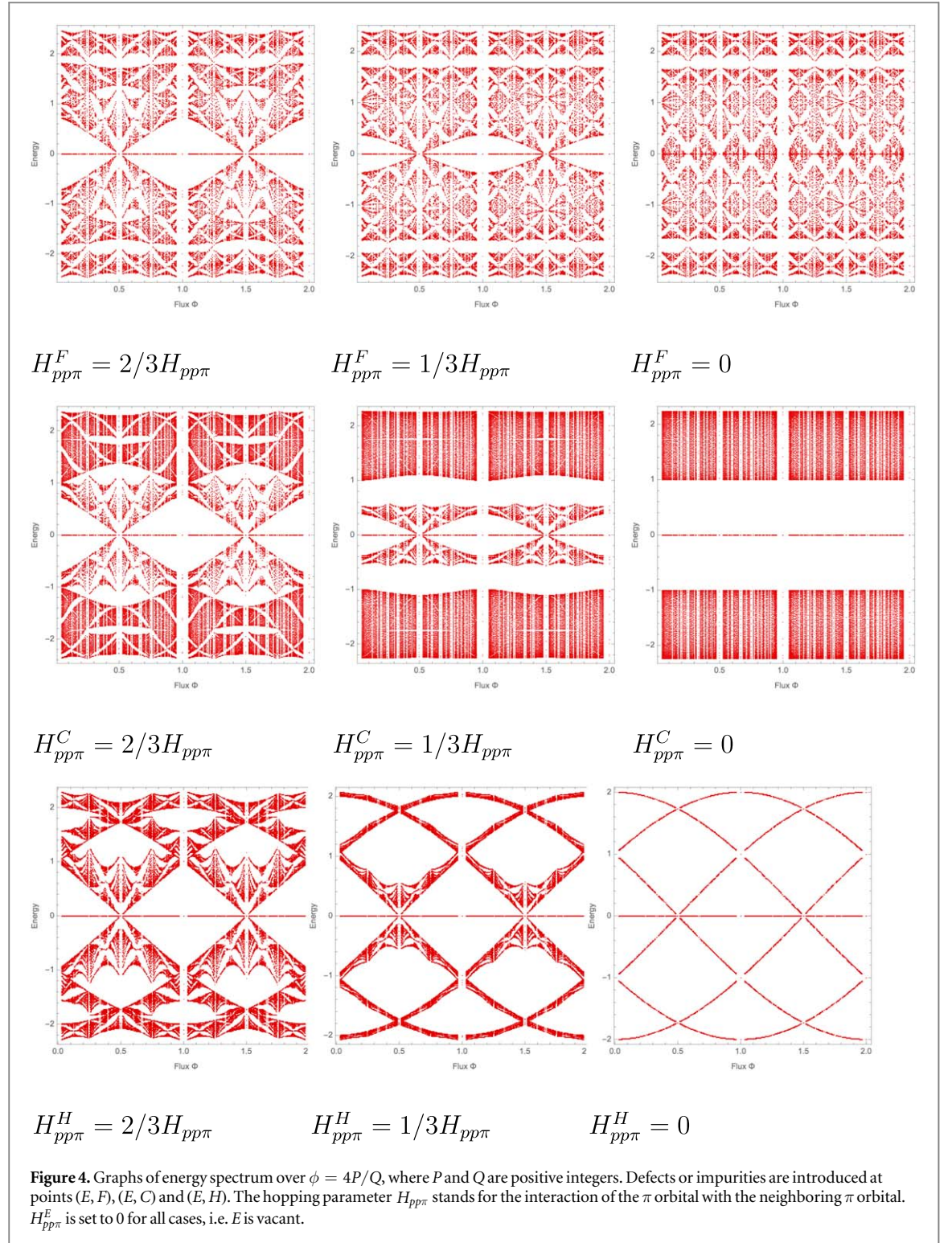
3.1.2 defects in a unit cell

We begin with the case where a single defect exists at E in a unit cell (figure 3). Compared with studies on Hofstadter's butterfly on a perfect lattice, a similar fractal nature can be found. Note that there are gapless points at $\phi = k + 1/2$ ($k \in \mathbb{N}_{\geq 0}$) in the $E = 0$ eV line and large band gaps having triangular shapes whose boundaries are formed by cos curves are formed elsewhere.

We next leave the atom at E vacant and introduce additional impurities or defects. Graphs of the spectrum over a wide range of rational magnetic fields ϕ are displayed in figure 4. We denote by $H_{pp\pi}^F$ the interaction of the π orbital of the atom at F with the neighboring π orbital. We first consider the case where an impurity is inserted at F . According to the figures in figure 4, there are three different patterns based on positions of impurities. As interactions with the atom E get weakened ($H_{pp\pi}^F \rightarrow 0$), energy levels split and form gaps around $|E| \sim 1.8$ eV. Consequently, energy levels within ± 1.8 eV ranges are modified and the blank area having a bicone shaped energy gap within $|E| < 1.0$ eV shrinks. If atoms at E and F are missed, then the graph acquires a new transition symmetry whose period is one-quarter of the original. When only a single impurity exists in a unit cell, those central band gaps are robust: it does not disappear for arbitrary non-zero value of hopping parameter $H_{pp\pi}^E$ [18]. However this is not true if additional impurity is considered.

In contrast to this case, flow of spectra formed in the process of $H_{pp\pi}^C \rightarrow 0$ show completely different behavior. As seen in the figures of $H_{pp\pi}^C$, the arcwise sets of spectra in figure 3 becomes boundaries which divide the chunks of spectra into three parts. As a result, all spectra within the range $|E| < 0.8$ eV in the figure of $H_{pp\pi}^C = 1/3 H_{pp\pi}$ approach to $E = 0$ eV, namely the corresponding states get degenerated, and the graph of $H_{pp\pi}^C = 0$ does not accommodate any fractal nature. Though there is a wide band gap in $|E| \leq 1$ eV, the other regions are gapless. This is in contrast to the case $H_{pp\pi}^F = 0$, which has band gaps around $|E| = 1.8$ eV. Note that when atoms at E and C are missed, then the honeycomb lattice is no more arcwise connected and the boundaries are zigzag. Therefore one may naively think that this is consistent with the fact that Hofstadter's butterfly never appears on any one-dimensional lattice system, but this is not correct here. To confirm this, we also tried a case with armchair boundaries and as a result, we obtained graph which exhibits the fractal nature (figure 5).

The last case $H_{pp\pi}^H \rightarrow 0$ is also different from the above two cases. Energy bands localize around six independent stripes (or cos curves) which remain at $H_{pp\pi}^H = 0$. They would correspond to energy bands of the six atoms living in the unit cell. It should be noted that there are band crossing points in the $E = 0$ eV line throughout the process, and the fractal nature of graphs also observed for all non-zero $H_{pp\pi}^H$.



3.2. Dependence on the size of unit cells

We next consider the unit cell size dependence of the energy spectrum. To address this problem, we extend the previous unit cell which contains 8 atoms as shown in figure 2. The graphs of spectrum on unit lattice (b) in figure 2 with a single defect correspond to (b-1) and (b-2) in figure 6, and similarly defined for spectra on unit cell (c). Fractal structures can be found in either case. One significant aspect is that there are robust gapless points ($\phi = 0.5$ for example) in the $E = 0$ eV line even if a single defect is inserted in a unit cell, without depending on its size (see (b-2) and (c-2) for detail). Those points exist in the Hofstadter problem on both the perfect honeycomb lattice (figure 1) and in the previous case with a defect at E (figure 3). In Hofstadter's original case on a square lattice, those points also correspond to the center of butterflies and their basic shapes are protected (compare also with figure 4) unless the fractality is lost. Therefore it would be natural to guess that such a gapless

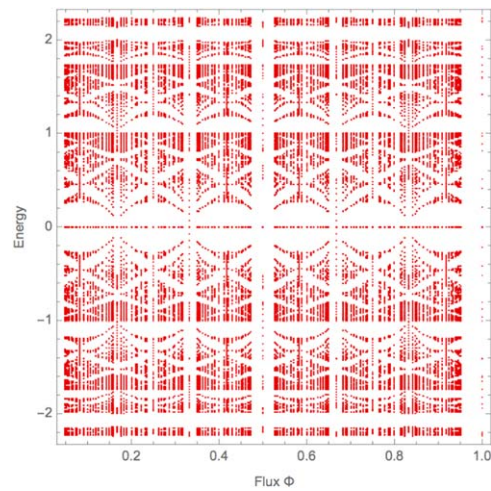
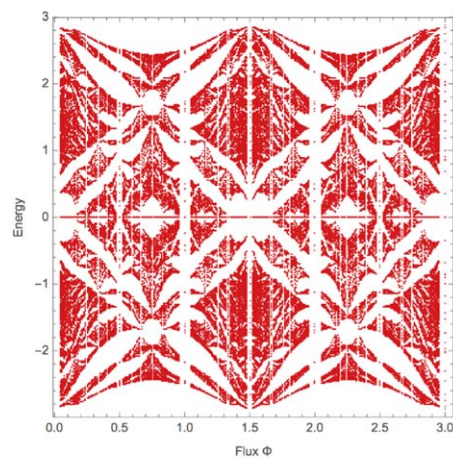
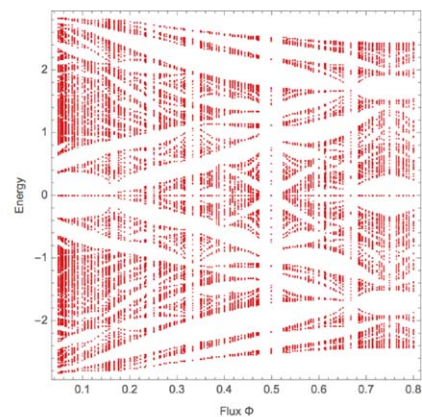


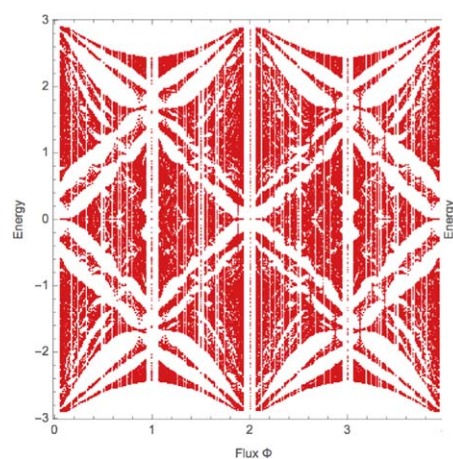
Figure 5. Butterflies on the honeycomb lattice with armchair boundaries. We use the lattice (b) in figure 2 cut along A, E, F, M, N, R .



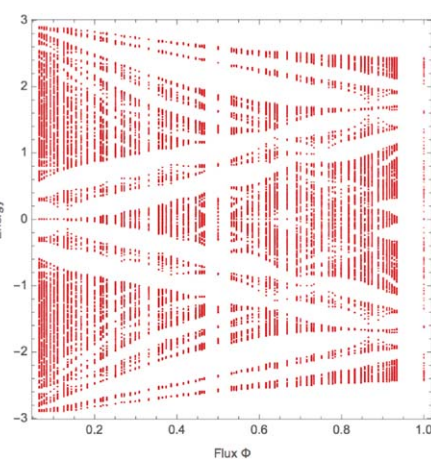
(b-1)



(b-2)



(c-1)



(c-2)

Figure 6. Spectra on the different enlarged unit cells. (b-1) corresponds to a two-period of the energy spectra considered on the unit cell (b) in figure 2 and the area around $\phi = 0.5$ is picked up and displayed in (b-2). (c-1) and (c-2) are labeled in a same manner.

point exist without depending on lattice forms, and this gapless point always appear if the graph has the fractality. This fact is very particular since the other gapless points (ex. $\phi = 0.25$ in figure 1) which exist in the perfect lattice case disappear when there is a defect in a unit cell.

4. Conclusion and future works

In this note, we considered the Hofstadter problem on the honeycomb lattice with defects using the tight-binding Hamiltonian including the nearest-neighbor interactions. We examined the contributions from defects or impurities to the formulation of Hofstadter's butterfly. Naively, increasing the number of defects in a unit cell makes graphs less fractal. However we found a case where it recovers its fractal nature and acquires a new translation symmetry. In addition, we also surveyed the dependence on the size of unit cells with a single defect and unexpectedly found robust gapless points in the $E = 0$ eV line. Those points exist without depending on the size of a unit cell and they exist at the center of butterflies. Therefore we may conclude that the butterfly at $\phi = 0.5$ point is immortal as long as graphs have fractal structures. In the end we add some comments on experimental study. A few experimental efforts to detect the Hofstadter butterflies have been reported. Measurements of the quantized Hall conductance in such a structure indirectly suggest the complex pattern of gaps that was expected in the butterfly spectrum [21, 22], for example. Most recently, a direct measurement technique of the fractal energy spectrum using a chain of 9 superconducting qubits were proposed [23], in which disorder was introduced to study the statistics of the energy levels of the system as it undergoes the transition from a thermalized to a localized phase. By applying this method, it will be possible to observe the main features of the intricate energy spectrum predicted in this article for two-dimensional lattice system with a number of defects in a magnetic field. Our results show that the fractal nature of energy spectrum is rather robust against the presence of defects or impurities, thereby it will be experimentally easier to observe butterflies compared to a study on a perfect lattice, which is difficult to prepare.

For future work, there are several research direction. It will be interesting to investigate the defect dependence of the fractality in other lattices such as triangular lattice and square lattice. Moreover it is also possible to consider Hamiltonian with the next-nearest-interactions. We found that the choices of missing two points are crucial to energy structures. But we also admit that interactions among Bloch wave functions are also crucial. It would be also intriguing to find a topological method to describe butterflies with or without defects. Especially we are curious how the robustness of the gapless points can be described in a more theoretical way. When a standard topological insulator has a gapless point, then its topological number usually change there. We expect there would be a certain topological number whose parameter is ϕ . Moreover, extension to higher dimensional case remains open question. Does such a robust gapless point generally exist in higher dimensional lattice spaces? If so, does it depend on space's dimension? How can it be generically described in a uniformed manner?

ORCID iDs

Kazuki Ikeda  <https://orcid.org/0000-0003-3821-2669>

References

- [1] Hofstadter D R 1976 Energy levels and wave functions of bloch electrons in rational and irrational magnetic fields *Phys. Rev. B* **14** 2239–49
- [2] Dean C R *et al* 2013 Hofstadter's butterfly and the fractal quantum hall effect in moiré superlattices *Nature* **497** 598 EP –
- [3] Ponomarenko L A *et al* 2013 Cloning of dirac fermions in graphene superlattices *Nature* **497** 594 EP –
- [4] Hunt B *et al* 2013 Massive dirac fermions and hofstadter butterfly in a van der waals heterostructure *Science* **340** 1427–30
- [5] Yilmaz F and Oktel M Ö 2017 Hofstadter butterfly evolution in the space of two-dimensional Bravais lattices *Phys. Rev. A* **95** 063628
- [6] Apalkov V M and Chakraborty T 2015 Fractal butterflies in buckled graphenelike materials *Phys. Rev. B* **91** 235447
- [7] Hatsugai Y and Kohmoto M 1990 Energy spectrum and the quantum hall effect on the square lattice with next-nearest-neighbor hopping *Phys. Rev. B* **42** 8282–94
- [8] Hatsuda Y, Katsura H and Tachikawa Y 2016 Hofstadter's butterfly in quantum geometry *New J. Phys.* **18** 103023
- [9] Hatsuda Y, Sugimoto Y and Xu Z 2017 Calabi-Yau geometry and electrons on 2d lattices *Phys. Rev. D* **95** 086004
- [10] Ikeda K 2018 Hofstadter's butterfly and langlands duality *J. Math. Phys.* **59** 061704
- [11] Ikeda K 2018 Quantum hall effect and langlands program *Ann. Phys., NY* **397** 136–50
- [12] Ikeda K Topological aspects of matters and langlands program arXiv:1812.11879 [cond-mat.mes-hall]
- [13] Koshino M, Aoki H, Kuroki K, Kagoshima S and Osada T 2001 Hofstadter butterfly and integer quantum hall effect in three dimensions *Phys. Rev. Lett.* **86** 1062–5
- [14] Brüning J, Demidov V V and Geyler V A 2004 Hofstadter-type spectral diagrams for the bloch electron in three dimensions *Phys. Rev. B* **69** 033202
- [15] Kimura T 2014 Hofstadter problem in higher dimensions *Progress of Theoretical and Experimental Physics* **2014** 103B05
- [16] İslamoğlu S, Oktel M Ö and Gülseren O 2012 The integer quantum hall effect of a square lattice with an array of point defects *J. Phys.: Condens. Matter* **24** 345501
- [17] İslamoğlu S, Oktel M Ö and Gülseren O 2013 Hall conductance in graphene with point defects *J. Phys.: Condens. Matter* **25** 055302
- [18] İslamoğlu S, Oktel M Ö and Gülseren O 2012 Hofstadter butterfly of graphene with point defects *Phys. Rev. B* **85** 235414
- [19] Peierls R 1933 Zur theorie des diamagnetismus von leitungselektronen *Zeitschrift für Physik* **80** 763–91

- [20] Harper P G 1955 The general motion of conduction electrons in a uniform magnetic field, with application to the diamagnetism of metals *Proceedings of the Physical Society. Section A* **68** 879
- [21] Geisler M C, Smet J H, Umansky V, von Klitzing K, Naundorf B, Ketzmerick R and Schweizer H 2004 Detection of a landau band-coupling-induced rearrangement of the hofstadter butterfly *Phys. Rev. Lett.* **92** 256801
- [22] Albrecht C, Smet J H, von Klitzing K, Weiss D, Umansky V and Schweizer H 2001 Evidence of hofstadter's fractal energy spectrum in the quantized hall conductance *Phys. Rev. Lett.* **86** 147–50
- [23] Roushan P *et al* 2017 Spectroscopic signatures of localization with interacting photons in superconducting qubits, *Science* **358** 1175